Reaction of the *Z* Isomer of 4-*trans*-(*N*,*N*-Dimethylamino)cinnamaldoxime with the Liver Alcohol Dehydrogenase–Oxidized Nicotinamide Adenine Dinucleotide Complex†

Mohamed A. Abdallah, Jean-François Biellmann,* Eila Cedergren-Zeppezauer, Martin Gerber, Helmut Dietrich,‡ Michael Zeppezauer,* Steven C. Koerber,§ Alastair K. H. MacGibbon,‖ and Michael F. Dunn*

ABSTRACT: The *Z* isomer of 4-*trans*-(*N*,*N*-dimethylamino)-cinnamaldoxime, (*Z*)-DMOX ($\lambda_{max}^{H_2O}$ 354 nm), forms a ternary complex with NAD^+ and equine liver alcohol dehydrogenase. The 3-acetyl (3-acetyl-$PdAD^+$), 3-thiocarboxamide (3-thio-NAD^+), 3-iodo (io^3$PdAD^+$) and nicotinamide mononucleotide (NMN^+) analogues of NAD^+ also form ternary complexes with enzyme and (*Z*)-DMOX. These complexes are characterized by large red-shifts in the UV–visible spectrum of bound (*Z*)-DMOX (λ_{max} 428 nm for the NAD^+ complex) and new spectral bands in the 280–340-nm region associated with the pyridine moieties of NAD^+ and the NAD^+ analogues. The ternary enzyme–NAD^+–(*Z*)-DMOX complex is weakly fluorescent (λ_{ex} 430 nm; λ_{em}^{max} 505 nm) and strongly quenches the residual tryptophan fluorescence of the enzyme–NAD^+ binary complex. (*Z*)-DMOX binds with high affinity to the enzyme–NAD^+ complex ($K_d \leq 4 \times 10^{-9}$ M at pH 8.75 and 25 °C), and similarly high affinities were found for the 3-acetyl-$PdAD^+$, 3-thio-NAD^+, and io^3$PdAD^+$ complexes. Binding is much weaker to the enzyme–NMN^+ complex. The active site specifically substituted Co(II), Ni(II), Cu(II), and Cd(II) enzyme derivatives and the enzyme species lacking any metal ion at the active site (apoenzyme) also form ternary complexes with (*Z*)-DMOX in which the DMOX UV–visible spectrum is red-shifted (ranging from 43 to 83.5 nm). The complexes formed with the Zn(II) and Co(II) enzymes are characterized by relatively high affinities for (*Z*)-DMOX and by spectra that are independent of pH over the range 6–10. The affinity of the apoenzyme–NAD^+ complex for (*Z*)-DMOX is much lower, and the spectrum of the complex is pH dependent with λ_{max} = 430 nm at pH 7 and λ_{max} = 397 nm at pH 10. The rate of (*Z*)-DMOX dissociation from the apoenzyme complex was found to be $\sim 10^3$-fold greater than the rates observed for the metal ion substituted enzymes. The 280–340-nm spectral bands appear to result from the dihydropyridine moieties of covalent adducts formed between (*Z*)-DMOX and NAD^+ and the NAD^+ analogues. The large red-shifts of the (*Z*)-DMOX spectrum result from the bonding of the oxime nitrogen to a strong electrophilic center (either the active site zinc ion or the nicotinamide ring of NAD^+). Attempts to fit these structures into the three-dimensional structure of the E(NADH,Me_2SO) complex via model building indicate coordination of the oxime nitrogen to zinc and covalent bond formation between the oxime oxygen and C-4 of the nicotinamide ring. The high affinities and slow rates of dissociation of the metal-substituted enzyme complexes are due in part to the coordination of (*Z*)-DMOX to the active site metal, an interaction that is not possible for the apoenzyme complex.

The zinc-requiring alcohol dehydrogenases from liver exhibit the unusual property of forming tightly bound ternary complexes with NAD^+ and a wide variety of small molecules and anions, for example, cyanide ion, thiolate anions, hydroxylamine, hydrazine, aliphatic oximes, and pyrazole (Shifrin & Kaplan, 1960; Kaplan & Ciotti, 1954; Kaplan, 1960; Theorell & Yonetani, 1963; Sund & Theorell, 1963; Sigman et al., 1982). The nucleophilic properties and/or ability to coordinate metal ions are the only obvious features common to these inhibitors. The kinetics of complex formation are more complicated than a simple binding reaction. The formation rates are slower than diffusion-limited rates by several orders of magnitude (McFarland & Bernhard, 1972; Andersson et al., 1981; Shore & Gilleland, 1970; Sigman et al., 1982; M. F. Dunn, unpublished results). The dissociation rates are generally very slow. Complex formation is accompanied by the appearance of a new UV spectral band located in the 280–360-nm region. The band widths, energies, and extinction coefficients of these spectral bands are similar to the long-wavelength electronic transition of enzyme-bound NADH.[1]

† From the Institut de Chimie (Laboratoire associé au C.N.R.S.), Universite Louis Pasteur de Strasbourg, Strasbourg, France (M.A.A. and J.-F.B.), The Swedish University of Agricultural Sciences, 75007 Uppsala 7, Sweden (E.C.-Z.), the Fachbereich 15.2, Analytische und Biologische Chemie, Universität des Saarlandes, Saarbrücken, West Germany (M.G., H.D., and M.Z.), and the Department of Biochemistry, University of California, Riverside, Riverside, California 92521 (S.C.K., A.K.H.M., and M.F.D.). *Received March 7, 1983; revised manuscript received September 23, 1983.* This work was supported by National Science Foundation Grants PCM 79-11526 and PCM 8108862, grants from the Deutsche Forschungsgemeinschaft (Ze 152/7), the Fonds der Chemischen Industrie, and the Fondation pour La Recherche Medicale, and Swedish Science Research Council Grant 2767.

‡ Present address: Department of Biochemistry and Biophysics, School of Medicine, University of California, San Francisco, San Francisco, CA 94143, and Molecular Biology Division, Veterans Administration Medical Center, San Francisco, CA 94121.

§ Present address: Institut für Weinchemie und Getraenkeforschung Forschungsanstalt Geisenheim, 6222 Geisenheim, West Germany.

‖ Present address: Department of Chemistry, Biochemistry and Biophysics, Massey University, Palmerston North, New Zealand.

[1] Abbreviations: NAD^+ and NADH, oxidized and reduced nicotinamide adenine dinucleotide; (*E*)- and (*Z*)-DMOX, the *E* and *Z* isomers of 4-*trans*-(*N*,*N*-dimethylamino)cinnamaldoxime; LADH or enzyme, horse liver alcohol dehydrogenase; apoenzyme or apo-E, liver alcohol dehydrogenase lacking the two active site zinc ions but retaining the two structural zinc ions; Zn(II)-, Co(II)-, Ni(II)-, Cu(II)-, and Cd(II)E, the active site specific metal ion substituted enzyme derivatives; pyr, pyrazole; DACA, 4-*trans*-(*N*,*N*-dimethylamino)cinnamaldehyde; 3-acetyl-$PdAD^+$, 3-thio-NAD^+, and io^3$PdAD^+$, the 3-acetyl, 3-thiocarboxamide, and 3-iodopyridine analogues of NAD^+; NMN^+, nicotinamide adenine mononucleotide; H_2NADH, 1,4,5,6-tetrahydronicotinamide adenine dinucleotide; IBA, isobutyramide; CDI, 1,1′-carbonyldiimidazole; LDH, porcine lactate dehydrogenase; TES, 2-[[tris(hydroxymethyl)methyl]-amino]ethanesulfonic acid; TAPS, 3-[[tris(hydroxymethyl]methyl]-amino]propanesulfonic acid; NMR, nuclear magnetic resonance.

0006-2960/84/0423-1003$01.50/0

This absorption band arises from the π,π^* transition of the 1,4-dihydronicotinamide moiety. Consequently, it generally has been assumed that these inhibitors form complexes at the catalytic site via nucleophilic attack of the inhibitor (R–X–H) on the nicotinamide ring of NAD^+ to give a covalent adduct (eq 1). Those inhibitors with bidentate character may form

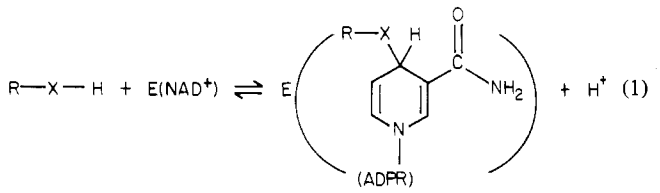

an additional stabilizing interaction via coordination to the active site zinc ion (Sund & Theorell, 1963), and X-ray structure studies (Eklund et al., 1982) show this to be the case for the E(NAD^+,pyr) adduct. Formation of such adducts is consistent with the chemical properties of NAD^+ (Kosower, 1962; Sund & Theorell, 1963; Siegel et al., 1959).

In this work, we present detailed UV–visible spectroscopic studies of the ternary complexes formed in the reaction of the *Z* isomer of 4-*trans*-(*N*,*N*-dimethylamino)cinnamaldoxime, (*Z*)-DMOX, with the Zn(II)E(NAD^+) complex and with Zn(II)E-bound NAD^+ analogues. We also present experiments with LADH species lacking the active site zinc ions and with various active site specific metal ion substituted derivatives. As will be shown, the spectroscopic properties and thermodynamic/kinetic behavior of these complexes provide evidence for (a) a strong bonding interaction between an electrophilic center at the site and the oxime nitrogen of (*Z*)-DMOX and (b) the formation of a covalent bond between (*Z*)-DMOX and the nicotinamide ring of NAD^+.

Materials and Methods

Materials. The 3-acetyl and 3-thiocarboxamide analogues of NAD^+ (3-acetyl-$PdAD^+$ and 3-thio-NAD^+) and nicotinamide adenine mononucleotide (NMN^+) (Sigma) and NAD^+ (grade I) and NADH (grade I) (Boehinger, Mannheim) were used without further purification. Native Zn(II)-substituted LADH (Boehringer, Mannheim) was prepared as previously described (Bernhard et al., 1970) except that the enzyme was extensively dialyzed against either 0.1 M pyrophosphate buffer, pH 8.75, or 0.1 M phosphate buffer, pH 7.5, to remove as much ethanol as possible. The metal ion substituted LADH species and apo-E were prepared as described by Maret et al. (1979), Andersson (1980), and Dietrich et al. (1983). Assays were carried out as previously described (Maret et al., 1979; Dunn et al., 1982). Most of the work reported with the Co(II)-, Ni(II)-, and Cd(II)-substituted enzyme derivatives used in these studies involved the same stock solutions used in the work reported by Dunn et al. (1982). On the basis of total protein concentration, the metal ion substituted enzymes had the following percentages of the active sites substituted: Co(II)E, ≥70%; Ni(II)E, ≥27%; Cu(II)E, ≥85%; Cd(II)E, ≥50%. The remainder of the protein consisted of apoenzyme with traces of denatured enzyme (≃0.5%) and trace amounts of Zn(II)-substituted enzyme. The Cu(II)E was prepared essentially as described by Maret et al. (1980): apo-E crystals in 0.033 M potassium–TES buffer, pH 6.9, were incubated for 48 h with a 5-fold excess of $CuSO_4$ and a 10-fold excess of ethylenediamine. After incubation, the excess Cu(II) was removed by dialysis. The yield of Cu(II)E sites was determined by using $\epsilon_{632} = 4800\ M^{-1}\ cm^{-1}$. The apo-E preparations used in these studies gave residual activities between 0.1 and 0.3% when compared with the native zinc enzyme. Porcine muscle lactate dehydrogenase and sodium pyruvate (Boehringer Mannheim) were used without further purification. The io^3PdAD^+ was prepared according to Abdallah et al. (1976). $^{15}NH_2OH$ HCl was purchased from C.E.A. (Saclay, France).

4-trans-(N,N-Dimethylamino)cinnamaldoxime, the Z and E Isomers. DACA (1.0 g) was dissolved in methanol (10 mL). Water (5 mL) was added and then sodium acetate (0.60 g) and finally hydroxylamine hydrochloride (1.0 g). The solution was refluxed 10 min and cooled, and the crystals were filtered to yield 0.95 g of a mixture of the *Z* and *E* isomers of the oxime. This was dissolved in a mixture of methylene chloride–diethyl ether (8:2), both freshly distilled, applied on a fine silica gel column (2.2 × 50 cm Kieselgel 60, 230–400 mesh, Merck), and chromatographed under pressure (5 atm), elution being with the same solvent mixture to yield 450 mg each of the *Z* and *E* isomers. (See Table I and Results for the assignment of stereochemistry.) For the *Z* isomer: mp 159 °C; λ_{max} (H_2O–0.1 M sodium pyrophosphate buffer, pH 8.75) 354 nm; ϵ_{max} $2.48 \times 10^4\ M^{-1}\ cm^{-1}$; TLC (silica gel) R_f 0.2 (pentane–ether, 1:1); ^1H NMR, see Table I. For the *E* isomer: mp 142 °C; λ_{max} (H_2O–0.1 M sodium pyrophosphate buffer, pH 8.75) 333 nm; ϵ_{max} $2.31 \times 10^4\ M^{-1}\ cm^{-1}$; TLC (silica gel) R_f 0.35 (pentane–ether, 1:1); ^1H NMR, see Table I.

4-trans-(N,N-Dimethyl[^{15}N]amino)cinnamaldoxime, the Z and E Isomer Mixture. This mixture was prepared by dissolving DACA (23 mg) in 1 mL of a CH_3CO_2H–$CHCl_3$ 9:1 mixture and adding successively $^{15}NH_2OH$ HCl (13 mg), sodium acetate (10 mg), and sodium (tri[$^2H_3$]methylsilyl)-propanesulfonate (2 mg); see Table I for the ^{15}N NMR of this mixture.

N-Phenyl-α-[2-[4-(Dimethylamino)phenyl]ethenyl]nitrone. This compound was prepared according to Boyland & Nery (1963) from DACA and *N*-phenylhydroxylamine. The nitrone had the following: mp 196 °C (lit. mp 203 °C); λ_{max} (ethanol) 436 nm; ϵ_{max} $3.80 \times 10^4\ M^{-1}\ cm^{-1}$. The ^1H NMR showed the presence of both the *Z* and *E* isomers.

Reactions of (Z)- and (E)-DMOX with 1,1'-Carbonyldiimidazole (CDI). The reactions of the *Z* and *E* isomers of DMOX were studied by observing the time courses of the reactions with a rapid-scanning (1 s/scan) HP8450A UV–visible spectrophotometer. Reaction was initiated by the addition of a 50-μL aliquot of a 5 mM oxime stock solution (CH_3CN) to a glass-stoppered cuvette containing a concentrated solution of CDI (~0.15 M) in 3 mL of dry CH_3CN (25 °C). The reaction of the *Z* isomer (see Results) was characterized by the rapid formation ($t_{1/2} \simeq 10$ s) of a species with a $\lambda_{max}^{CH_3CN}$ of 370 nm (presumed to be the *O*-acyl intermediate). This species then underwent a relatively rapid ($t_{1/2} \simeq 1$ min) conversion to a product ($\lambda_{max}^{CH_3CN}$ 360 nm) identified as 4-*trans*-(*N*,*N*-dimethylamino)cinnanonitrile by comparison of UV–visible spectra with an authentic sample.

The reaction of the *E* isomer was characterized by the rapid formation ($t_{1/2} \simeq 1$ min) of a species with a $\lambda_{max}^{CH_3CN}$ of 365 nm (presumed to be the *O*-acyl species). This species then underwent a relatively slow ($t_{1/2} \simeq 20$ min) transformation to a final product with a $\lambda_{max}^{CH_3CN}$ of 365 nm (presumed to be the *O*-acyl species). This species then underwent a relatively slow ($t_{1/2} \simeq 20$ min) transformation to a final product with a $\lambda_{max}^{CH_3CN}$ of 342 nm. This product was not identified.

UV–Visible and Fluorescence Spectral and Kinetic Measurements. The UV–visible spectra were measured on either a Varian 635 UV–visible recording spectrophotometer with tandem cuvettes (total path length 0.876 cm) or a Hewlett-Packard 8450A rapid-scanning spectrophotometer. The visible

Table I: ^{1}H NMR Data for the *Z* and *E* Isomers of 4-*trans*-(*N*,*N*-Dimethylamino)cinnamaldoxime

	chemical shifts from tetramethylsilane (ppm)[a]					
	H_1	H_2	H_3	*o*,*o*′	*m*,*m*′	$N(CH_3)_2$
Z (mp 159 °C)	7.17	7.22	6.80	7.438	6.70	2.96
E (mp 142 °C)	7.80	6.55	6.79	7.30	6.70	2.96

	coupling constants (Hz)				
	$J_{1,2}$	$J_{2,3}$	$J_{o,m}$	$J_{^{15}N,1}$[b]	$J_{^{15}N,2}$[b]
Z (mp 159 °C)	15	9.3	9	-14.5	-2.0
E (mp 142 °C)	16	9.5	9	3	-2.0

[a] Spectra were measured at 20 °C in CH_3CO_2H–$CHCl_3$ (9:1 mixture) with a 250-MHz Cameca instrument.

absorption spectra of the Co(II)E(NAD$^+$–(*Z*)-DMOX) complex (Figure 3A) were obtained with a rapid-scanning UV-visible spectrophotometer consisting of a Princeton Applied Research Model 1412 silicon photodiode array detector (1024 elements), the PAR OMA-2 LSI-11 microprocessor-based data acquisition system, and a modified Durrum D-110 stopped-flow rapid-mixing spectrophotometer (Koerber & Dunn, 1981; Koerber et al., 1983). The sample was illuminated with "white light" from a tungsten lamp. The kinetics of the dissociation of (*Z*)-DMOX from the ternary complexes with the metal-substituted enzyme derivatives and the native zinc enzyme were determined with Varian Techtron Model 635 or Hitachi 100-10 UV–visible spectrophotometers. The 15–25 data points were fitted to a single exponential function by nonlinear regression analysis with a Hewlett-Packard 9825A calculator. Stopped-flow, rapid-mixing techniques were used to measure the dissociation of (*Z*)-DMOX from the apo-E(NAD$^+$–(*Z*)-DMOX) complex by displacement with pyrazole via single-wavelength, stopped-flow methods (Dunn et al., 1979).

Fluorescence measurements were made with a double-monochromator Farrand MK-II recording fluorometer thermostated at 25.0 ± 0.2 °C. In all experiments (except those involving NMN$^+$), porcine muscle lactate dehydrogenase and sodium pyruvate were added to convert any reduced dinucleotide (formed via oxidation of trace contaminants of alcohol) back to the oxidized form. Absorbance and fluorescent titrations were carried out by adding small aliquots (10 μL) from a calibrated micrometer syringe assembly. Mixing was accomplished by bubbling air or nitrogen through the solution after each addition. Model-building experiments were carried out with a Vector General 3404 interactive graphics display by using the Alwyn Jones FRODO program (Jones, 1982).

Results

UV–Visible Spectral Properties of the Zn(II)E(Dinucleotide–(Z)-DMOX) Complexes. In agreement with the findings of Frölich (1977) and Sigman et al. (1982), the unresolved mixture of the *Z* and *E* isomers of 4-trans-(*N*,*N*-dimethylamino)cinnamaldoxime, (*Z*)- and (*E*)-DMOX, when mixed with the Zn(II)E(NAD$^+$) complex yields a species exhibiting a long-wavelength absorption band with a λ_{max} of 430 nm. Since the *Z* and *E* isomers might be expected a priori to behave differently within the confines of the LADH active site, the purified isomers (see Materials and Methods) were separated over silica gel under 5-atm pressure.

On the basis of ^{1}H NMR data alone (Table I), it was not possible to make an unambiguous assignment of the stereochemistry of these oximes. The coupling constant of the aldehydic proton with the ^{15}N of ^{15}N-enriched oximes has been shown to be a valuable tool for the determination of the stereochemistry of oximes (Kintzinger & Lehn, 1967; Crêpeaux & Lehn, 1975). Therefore, a mixture of the ^{15}N-enriched oximes was prepared with [^{15}N]hydroxylamine, and the ^{15}N–^{1}H coupling constants were determined (Table I). The compound (mp 159 °C) with the H_1 resonance at 7.17 ppm showed a *large negative* coupling constant and thus is the *Z* isomer; the compound (mp 142 °C) with the H_1 resonance at 7.80 ppm showed a *small positive* coupling constant and thus is the *E* isomer (Crêpeaux & Lehn, 1975).

Reaction of the two isomers with 1,1′-carbonyldiimidazole (CDI) provided an independent verification of these structural assignments. As expected, reaction of the *Z* isomer with CDI in dry acetonitrile resulted in the rapid ($t_{1/2} \simeq 1$ min), quantitative conversion of the oxime to the corresponding nitrile ($\lambda_{max}^{CH_3CN}$ 360 nm) (Foley & Dalton, 1973). Under identical experimental conditions, the *E* isomer underwent a slow ($t_{1/2} \simeq 20$ min) quantitative conversion to some other product ($\lambda_{max}^{CH_3CN}$ 342 nm). The identity of this product has not been established. The rapid conversion of (*Z*)-DMOX to the nitrile and the inability of (*E*)-DMOX to undergo this transformation are consistent with the well-known propensity exhibited by *O*-acyl derivatives of (*Z*)-aldoximes [but not (*E*)-aldoximes] to undergo facile elimination to the nitrile (Foley & Dalton, 1973; Chakrabarti & Hotten, 1972; Clive, 1970; Hill & Schomookler, 1967).

Our results agree in broad outline with the findings of Sigman et al. (1982) but not in every detail. For example, they report a synthesis involving slightly different conditions (i.e., heating DACA, hydroxylamine hydrochloride, and sodium acetate in aqueous ethanol) which, after recrystallization, apparently gave only (*Z*)-DMOX. The ^{1}H NMR of this compound is similar to that of our sample of (*Z*)-DMOX, but their product sintered at 164–166 °C and melted at 171–173 °C, whereas our (*Z*)-DMOX sample melts sharply at 159 °C. They report a $\lambda_{max}^{H_2O}$ of 350 nm, in good agreement with our value of 354 nm, but they show a spectrum (their Figure 7) with λ_{max} near 335 nm, similar to that of our *E* isomer. We conclude that these minor differences arise primarily from the slow (probably light-catalyzed) interconversion of the *Z* isomer to the *E* isomer (see Discussion).

When the purified isomers were mixed in separate experiments with the LADH(NAD$^+$) complex, only the *Z* isomer gave the red-shifted complex. With (*Z*)-DMOX concentrations in the 10–100 μM range, reaction is complete within 10 s. The *E* isomer (as judged by the absence of spectral changes) does not appear to interact in any way with the LADH-(NAD$^+$) complex. For example, no spectral changes were observed over a time period of 2 h. Further studies showed that a variety of NAD$^+$ analogues could substitute for NAD$^+$ in the reaction with (*Z*)-DMOX but that neither the LADH-(NADH) complex nor coenzyme-free enzyme gives chromophoric complexes.

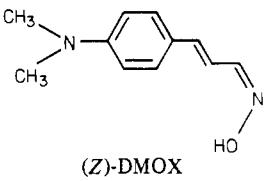

(*Z*)-DMOX

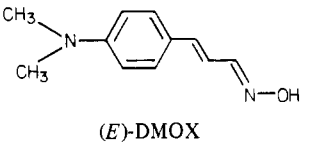

(*E*)-DMOX

The results of UV–visible spectral investigations of the NAD$^+$ complex and the complexes involving Zn(II)E and 3-acetyl-PdAD$^+$, 3-thio-NAD$^+$, and io^{3}PdAD$^+$ are shown in Figure 1. (*Z*)-DMOX was found to bind to the NAD$^+$, 3-thio-NAD$^+$, and 3-acetyl-PdAD$^+$ Zn(II)E complexes with relatively high affinity and with a stoichiometry of one complex

Table II: UV-Visible Spectral Properties of the Ternary Complexes Formed between (*Z*)-DMOX, LADH, NAD^+, and Various NAD^+ Analogues[a]

NAD^+ analogue	absorption bands[b]				difference spectra[b]					
	λ_{max}	ϵ_{max}	λ_{max}	ϵ_{max}	λ_{max}	$\Delta\epsilon_{max}$	λ_{min}	$\Delta\epsilon_{min}$	λ_{max}	$\Delta\epsilon_{max}$
NAD^+	290	1.37×10^4	428	4.21×10^4	287	7.76×10^3	347	-2.13×10^4	429	3.97×10^4
3-acetyl-$PdAD^+$	305	1.93×10^4	432	4.07×10^4	293	5.52×10^3	348	-1.72×10^4	432	3.96×10^4
3-thio-NAD^+	335	1.60×10^4	428	4.15×10^4			363	-1.21×10^4	430	3.94×10^4
io^3PdAD^+[c]			427	3.57×10^4	<300		348	-1.63×10^4	430	3.23×10^4
NMN^+			430				345		428	

[a] Determined in pH 8.75 sodium pyrophosphate buffer, 10 mM, at 25.0 ± 0.2 °C (see Figures 1 and 2 for experimental details). [b] Due to the number and intensity of chromophores present, meaningful spectral measurements could not be made in the region below ~280 nm. λ_{max} and λ_{min} values are in nanometers. ϵ_{max} and ϵ_{min} values are in M^{-1} cm^{-1}. [c] Due to the absorbancies of enzyme, io^3PdAD^+, and (*Z*)-DMOX, meaningful measurements could not be made in the region below 300 nm.

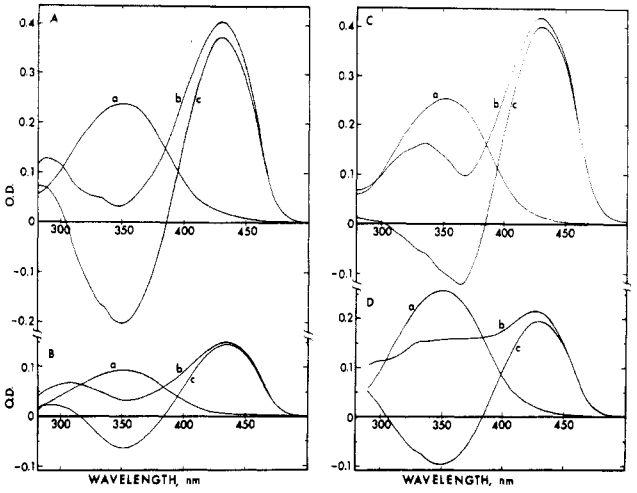

FIGURE 1: Spectra and difference spectra of the ternary complexes formed in the reactions of (*Z*)-DMOX with NAD^+ and NAD^+ analogues bound to LADH. The coenzymes used are as follows: (A) NAD^+, (B) 3-acetyl-$PdAD^+$, (C) 3-thio-NAD^+, and (D) io^3PdAD^+. Each set of spectra contains, respectively, (a) the spectrum of free (*Z*)-DMOX, (b) the spectrum of the ternary complex minus the spectra of LADH and coenzyme, and (c) the difference spectrum consisting of the ternary complex minus the spectrum of free (*Z*)-DMOX. All the spectra were measured by using tandem cuvettes (total path length 0.872 cm) according to the following procedures: 1.00-mL aliquots containing the desired amounts of LADH, NAD^+, or NAD^+ analogue, 1 mM sodium pyruvate, and a trace of LDH were added to the first compartment each of the reference and sample cuvettes, and 1.00 mL of buffer was added to the second compartment of each cuvette; then, the base line was measured. To measure the spectrum of (*Z*)-DMOX (spectrum a), 10 μL of buffer was withdrawn from the second compartment of the sample cuvette and replaced by a 10-μL aliquot of concentrated (*Z*)-DMOX (in CH_3CN), and the resulting spectrum was recorded. The spectrum of the ternary complex (spectrum b) was obtained after mixing the contents of the two compartments of the sample cuvette. The difference spectrum (spectrum c) was measured after adding 10 μL of (*Z*)-DMOX to the buffer compartment of the reference cuvette (after first withdrawing 10 μL of buffer). To check the precision of the pipetting, the reference cuvette was then mixed and a final base line recorded. In all of the experiments reported, the final base line was found to be identical with the initial base line (within the limits of instrument reproducibility). Conditions after mixing were as follows: (A) [LADH] = 18.1 μN, [NAD^+] = 0.5 mM, and [(*Z*)-DMOX] = 10.5 μM; (B) [LADH] = 10.2 μN, [3-acetyl-$PdAD^+$] = 0.42 mM, and [(*Z*)-DMOX] = 4.3 μM; (C) [NADH] = 14.7 μN, [3-thio-NAD^+] = 0.5 mM, and [(*Z*)-DMOX] = 11.3 μM; (D) [LADH] = 14.0 μN, [io^3PdAD^+] = 2.8 mM, and [(*Z*)-DMOX] = 12.5 μM. All spectra were measured in 0.1 M sodium pyrophosphate buffer, pH 8.75 at 25.0 ± 0.2 °C. (A–C) Measured in the presence of 0.5 mM sodium pyruvate and a trace of porcine lactate dehydrogenase (60 μg/mL) to ensure that the net conversion of oxidized coenzyme to reduced coenzyme via any "blank" reaction was negligible.

per subunit (see below). Virtually stoichiometric amounts of the NAD^+, 3-thio-NAD^+, and 3-acetyl-$PdAD^+$ complexes are formed under the conditions employed in parts A–C of Figure 1, respectively. The enzyme–io^3PdAP^+ complex binds (*Z*)-DMOX with a somewhat lower affinity, and under the conditions of Figure 1D, ternary complex formation is incomplete. Assuming identical and independent sites, analysis of binding titrations via Scatchard plots for the binding of (*Z*)-DMOX to the LADH (io^3PdAP^+) complex gave an extrapolated stoichiometry of one complex per subunit and an apparent dissociation constant $K_D \simeq 6$ μM. Each ternary complex is characterized by a red-shifted spectrum with an intense, long-wavelength, π,π^* absorption band ($\epsilon_{max} \simeq 4 \times 10^4$ M^{-1} cm^{-1}) derived from the (*Z*)-DMOX chromophore (Figure 1 and Table II). The position of this spectral band is only slightly dependent on the structure of the coenzyme (Figure 1, Table II). The NAD^+, 3-acetyl-$PdAD^+$, and 3-thio-NAD^+ complexes also give absorption bands in the 280–340-nm region. The position and intensity of these bands are markedly dependent on the structure of the NAD^+ analogue (Table II).

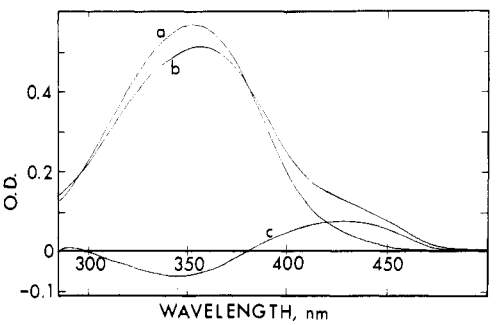

FIGURE 2: Spectra and difference spectra of the ternary complex formed between (*Z*)-DMOX and the LADH(NMN^+) complex. The spectra were measured as described in Figure 1. Conditions after mixing were as follows: [LADH] = 24.2 μN; [NMN^+] = 3.32 mM; [(*Z*)DMOX] = 25.3 μM; 0.1 M sodium pyrophosphate buffer, pH 8.75; 25.0 ± 0.2 °C.

Spectral Evidence for a Zn(II)E(NMN^+–(Z)-DMOX) Complex. β-Nicotinamide mononucleotide (NMN^+) also substitutes for NAD^+ in the formation of a red-shifted chromophore (Figure 2). However, the interaction between the Zn(II)E(NMN^+) complex and (*Z*)-DMOX is substantially weaker, and under the conditions used in Figure 2, ternary complex formation is incomplete. Consequently, the spectrum in Figure 2 has a large contribution from free DMOX (λ_{max} 354 nm) and a smaller contribution from the ternary complex (as evidenced by the 430-nm shoulder). The difference spectrum presented in Figure 2 indicates that the complex has a spectrum nearly identical in shape with the spectrum of the Zn(II)E(NAD^+–(*Z*)-DMOX) complex (Figure 1A). It was conceivable that the spectral band at ~430 nm actually arises from an NAD^+ impurity present in the NMN^+ sample. Therefore, a sensitive kinetic assay (Rasmussen et al., 1972) was employed to estimate an upper limit for the amount of NAD^+ present. The assay demonstrated that the NMN^+

Table III: Comparison of the Visible Spectral Properties of Selected 4-*trans*-(*N*,*N*-Dimethylamino)cinnamaldehyde Derivatives in LADH and Small Molecule Complexes

	M(II)E(NAD$^+$–(*Z*)-DMOX)			
metal ion	λ_{max} ($\Delta\lambda_{max}$) (nm)[a,b]	ϵ_{max}(app) ($\times 10^{-4}$ M^{-1} cm^{-1})	M(II)E(NADH–DACA) λ_{max} ($\Delta\lambda_{max}$) (nm)[a,c]	M(II)–VIII λ_{max} ($\Delta\lambda_{max}$) (nm)[a]
Co(II)	437 (83)	4.0	478 (80)	430[d] (56)
Ni(II)	437.5 (83.5)	4.4	475 (77)	415[d] (39)
Zn(II)	430 (76)	4.4	464 (66)	428[d] (54)
Cd(II)	428 (74)	3.8	457 (59)	416[e] (42)
Cu(II)	418 (64)	1.6		
none[f]	430 (76)	>2.5		

[a] $\Delta\lambda_{max} = \lambda_{max}$(complex) – λ_{max}(free), where λ_{max}(complex) is the λ_{max} of the (dimethylamino)cinnamyl chromophore in the complex and λ_{max}(free) is the λ_{max} of the free chromophore; λ_{max}(*Z*-DMOX) = 354 nm (aqueous solution, pH 4–10); λ_{max}(DACA) = 398 nm (aqueous solution, pH 4–10); λ_{max}(IV) = 374 nm (acetonitrile). [b] Determined in 4.5 mM TES buffer, pH 7.15, in solutions containing a large excess of NAD$^+$ (typically 1 mM) and with the concentration of metal ion substituted enzyme sites in slight excess of the total concentration of (*Z*)-DMOX. [c] Data taken from Dunn et al. (1982). [d] Data taken from Angelis et al. (1977). [e] M. F. Dunn, unpublished data. [f] The apo-E(NAD$^+$–(*Z*)-DMOX) complex measured at pH 7.5, see text and Figure 4.

sample contains no more than one molecule of NAD$^+$ per 7.28 $\times 10^6$ molecules of NMN$^+$. Therefore, the NMN$^+$ solution in Figure 2 could have contained no more than ~1.75 nM NAD$^+$. This concentration of NAD$^+$ could not account for the amount of 430-nm chromophore observed. In other UV–visible spectral studies (data not shown), attempts to demonstrate a ternary complex with enzyme, AMP, and (*Z*)-DMOX failed to give any indication of ternary complex formation.

UV–Visible Spectral Properties of the Ternary Complexes Formed with Metal Ion Substituted LADH Derivatives. The spectral properties of the complexes formed between (*Z*)-DMOX, NAD$^+$, and the Co(II)-, Ni(II)-, Cu(II)- and Cd(II) enzymes are given in Table III and Figure 3. The Co(II)E-(NAD$^+$–(*Z*)-DMOX) ternary complex exhibits a red-shifted spectrum [relative to free (*Z*)-DMOX] with a λ_{max} of 437 nm and apparent $\epsilon_{max} \simeq 4.0 \times 10^4$ M^{-1} cm^{-1} (Table III). The spectral changes associated with ternary complex formation for the Co(II)E, as measured by the d–d bands in the 500–700-nm region, are shown in Figure 3A. The Cd(II)E gives a ternary complex with (*Z*)-DMOX exhibiting a λ_{max} of 428 nm (Table III) and apparent $\epsilon_{max} \simeq 3.8 \times 10^4$ M^{-1} cm^{-1}, while the Ni(II)E gives a ternary complex with a λ_{max} of 437.5 nm and apparent $\epsilon_{max} \simeq 4.4 \times 10^4$ M^{-1} cm^{-1}. As has been previously documented (Maret et al., 1979; Dietrich et al., 1979; Maret, 1980; Dunn et al., 1982; Koerber et al., 1983), the d–d absorption bands of the Co(II)E are sensitive both to direct interactions between ligands and metal ion and to indirect interactions resulting from coenzyme binding [compare the spectra of Co(II)E and the ternary complex, Figure 3A].

The conditions employed in Table III and Figure 3 were found to give the ternary complexes in amounts that correspond to a 1:1 stoichiometry with the substituting metal ion. In the absence of NAD$^+$, the spectrum of (*Z*)-DMOX in solutions containing Ni(II)E is red-shifted by 5 nm (data not shown), indicating that a binary complex is formed with this enzyme species. Note that since ternary complex formation with the apo-E(NAD$^+$) complex is much weaker (K_D > 10 μM vs. $K_D \leq$ 10 nM), the spectra are unaffected by the presence of apo-E.

The UV–visible spectra of the Cu(II)E and the ternary Cu(II)E(NAD$^+$–(*Z*)-DMOX) complex are described in Table III and Figure 3B. The spectrum of the (*Z*)-DMOX chromophore with λ_{max} = 418 nm (apparent $\epsilon \simeq 1.6 \times 10^4$ M^{-1} cm^{-1}) is not as red-shifted. The broad envelope of absorption bands located between 500 and 800 nm (Figure 3B) consists of LMCT bands (Maret, 1980). The energies and intensities of these transitions are perturbed by the binding and reaction of NAD$^+$ and (*Z*)-DMOX. Upon formation of the complex

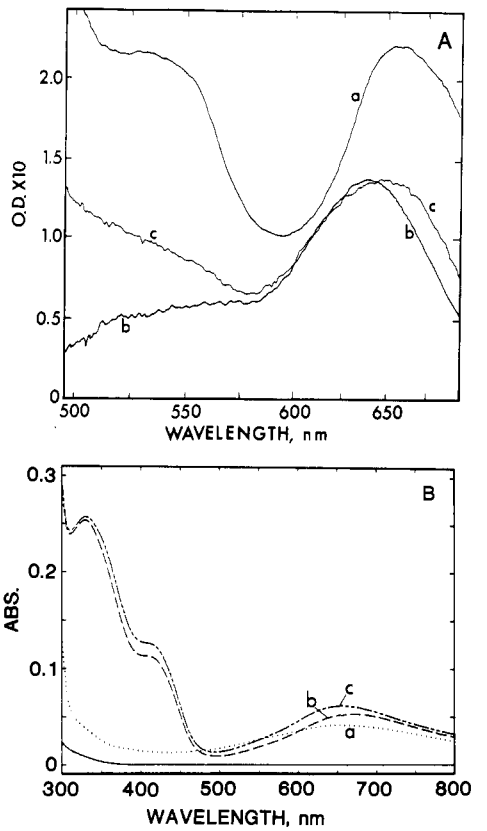

FIGURE 3: (A) Comparison of the d–d spectral bands of the Co(II)E(NAD$^+$–(*Z*)-DMOX) ternary complex (a) with the Co(II)E (b) and with the Co(II)E(NAD$^+$) binary complex (c) in 0.1 M sodium pyrophosphate buffer, pH 8.75, at 25 °C. The spectra were measured with a rapid-scanning stopped-flow spectrophotometer (see Materials and Methods). Trace a is the "infinite time" spectrum for the reaction of (*Z*)-DMOX with the Co(II)E(NAD$^+$) complex. Trace c is the spectrum collected 8 ms after mixing Co(II)E with the solution of NAD$^+$ and (*Z*)-DMOX, a time during which formation of the Co(II)E(NAD$^+$) binary complex is complete but the amount of 437-nm absorbing species formed is negligible. Trace b was measured in a separate experiment. Conditions were $[Co(II)E]_0 = 20$ μN throughout, $[NAD^+]_0 = 1$ mM, and $[(Z)\text{-DMOX}]_0 = 50$ μM. (B) UV–visible spectra of the Cu(II)E(NAD$^+$) complex (a) and the Cu(II)E-(NAD$^+$–(*Z*)-DMOX) complex at pH 7.0 (b) and 9.0 (c) at 25.0 ± 0.2 °C. (a) $[Cu(II)E]_0 = 13.9$ μN; $[NAD^+]_0 = 137$ μM; 0.1 M potassium–TES buffer, pH 7.0, $[KCl]_0 = 6$ mM. (b) Addition of 17.5 μM (*Z*)-DMOX to (a). (c) Same conditions as (b) but 0.1 M potassium glycinate buffer, pH 9.0.

at pH 7.0, the 640-nm envelope of the Cu(II)E shifts to 670 nm, and the intensity increases. At pH 9.0, the magnitude of the red-shift is smaller (~10 nm) but with a larger increase in intensity.

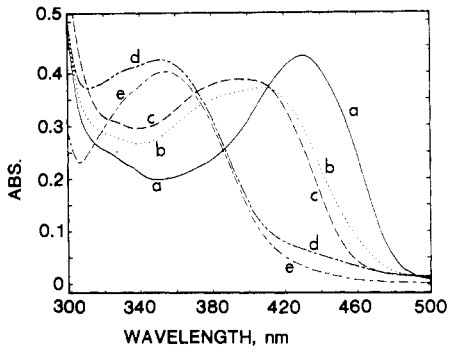

FIGURE 4: pH dependence of the spectra of the apo-E(NAD$^+$–(*Z*)-DMOX) complex at 25.0 ± 0.2 °C. (a) (—) Addition of 888 μM NAD$^+$, all in metal ion free 0.3 M TES–0.2 M TAPS buffer, pH 7.5, containing 10 μM EDTA. (b) (···) Same concentrations as (a) but 0.1 M sodium pyrophosphate buffer, pH 8.5. (c) (– –) Potassium glycinate buffer (0.1 M) pH 10.0. (d) (–·–·) Sodium acetate buffer (0.1 M), pH 5.0. (e) (– – –) $[\text{Apo-E}]_0$ = 35.5 μN; $[(Z)\text{-DMOX}]_0$ = 28.2 μM.

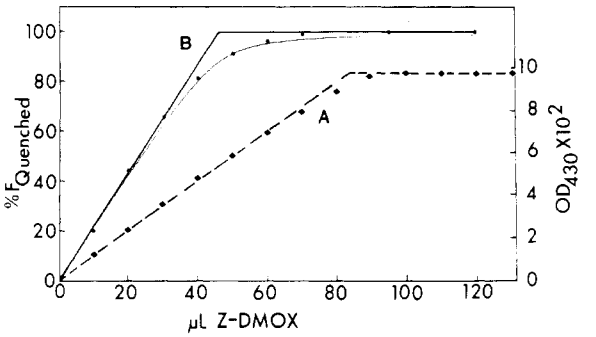

FIGURE 5: Titration of LADH sites as measured by the optical density charges at 430 nm (A) (♦) or by the quenching of enzyme fluorescence (B) (●) accompanying the formation of the LADH(NAD–(*Z*)-DMOX) ternary complex. Aliquots of a concentrated (*Z*)-DMOX solution (in buffer) were titrated into a cuvette containing LADH, NAD$^+$ sodium pyruvate, and LDH (at the desired concentrations) in 0.1 M sodium pyrophosphate buffer, pH 8.75, at 25.0 ± 0.2 °C. (A) Conditions were as follows: [LADH] = 2.7 μN (determined via the NAD$^+$–pyrazole assay; Theorell & Yonetani, 1963); [NAD$^+$] = 0.164 mM; [(*Z*)-DMOX stock solution] = 0.10 mM; [sodium pyruvate] = 1.7 mM; [LDH] = 50 μg/mL. The sodium pyruvate and LDH were added to render negligible the net conversion of NAD$^+$ to NADH via the "blank" reaction. The titration end point, 82 μL of (*Z*)-DMOX (end-point volume = 3.132 mL), yields a site concentration of 2.8 ± 0.3 μN. (B) The titration of LADH sites as measured by the quenching of the intrinsic protein fluorescence was carried out as in (A). Conditions after mixing were as follows: [LADH] = 0.3 μN (via the NAD$^+$–pyrazole assay; Theorell & Yonetani, 1963); [NAD$^+$] = 0.32 mM; [(*Z*)-DMOX stock solution] = 16.5 μM; [sodium pyruvate] = 0.78 mM; [LDH] ~ 4 μg/mL; 0.1 M sodium pyrophosphate buffer, pH 8.75, at 25.0 ± 0.2 °C. The titration end point, 46 μL of (*Z*)-DMOX, yields an active site concentration of 0.24 ± 0.03 μM. The curved line running through the data points is the computer-simulated theoretical fit under the assumptions (a) (*Z*)-DMOX binds to two identical and independent sites and (b) a titration end point of 46 μL (end-point volume = 3.206 mL) and with [LADH] = 0.236 μN and a K_D = 4 nM. Instrument settings were λ_{ex} 280 nm, λ_{em} 340 nm, and excitation and emission slits 10-nm band-pass.

In Table III where the concentrations of metal ion substituted sites are in slight excess over the concentration of (*Z*)-DMOX, formation of the ternary complexes appears to be essentially complete for all the derivatives with a stoichiometry of approximately 1:1 with the concentration of (*Z*)-DMOX. In no instance did the addition of more NAD$^+$ increase the amounts of ternary complex formed. The spectra of the complexes with the Zn(II)- and Co(II)-substituted enzymes are independent of pH over the pH range 6–10, whereas there appears to be a pH dependence to the spectrum of the Cu(II)E ternary complex (Figure 3B).

Evidence for an Apo-E(NAD$^+$–(Z)-DMOX) Ternary Complex. Efforts were made to evaluate the usefulness of the LADH–NAD$^+$–DMOX reaction as an analytical tool for detecting residual amounts of Zn(II) and/or other divalent metal ions at the enzyme active site in preparations of apo-E. These experiments resulted in the discovery that apo-E also forms a weakly bound ternary complex with (*Z*)-DMOX and NAD$^+$ (K_D > 10 μM). The spectrum of (*Z*)-DMOX in the apo-E(NAD$^+$–(*Z*)-DMOX) complex also is red-shifted (Figure 4, Table III). The spectrum of the complex undergoes reversible changes as a function of pH (Figure 4), and shifts from 430 nm at pH 7.5 to 397 nm at pH 10.0. (*Z*)-DMOX binds only weakly at pH 5. Under the conditions of Figure 4, binding is too weak to allow detection of the ternary complex by UV–visible spectroscopy below pH 5. Note that the pH 7.5 spectrum (λ_{max} = 430 nm) *is very similar* to that observed for the Zn(II)–, Co(II)–, Cd(II)–, and Ni(II)–enzyme systems, while the pH 10 spectrum (λ_{max} = 397 nm) shows a closer similarity to the spectrum of the Cu(II)E complex (λ_{max} = 418 nm). Because the apo-E is a relatively labile species, it was not possible to accurately determine either the (*Z*)-DMOX dissociation constant or the molar extinction coefficient for the complex. However, the spectrum presented in Figure 4 and titration studies (data not shown) indicate $\epsilon_{430} > 2.5 \times 10^4$ M^{-1} cm^{-1} and K_D > 10 μM. To determine whether or not the 430-nm spectral band actually is derived from (*Z*)-DMOX bound to apo-E(NAD$^+$) rather than to a metal ion contaminated apoenzyme preparation, some of the spectra (see Figure 4) were measured in the presence of 10 μM EDTA in a TES–TAPS buffer system as nearly completely free of *all* metal ions as we could achieve.

In control experiments, the apo-E preparation was found to retain only 2 mol of Zn(II) of the 4 mol of Zn(II)/80 000 daltons present in native LADH. These two remaining zinc ions have been shown to be bound almost exclusively to the structural sites (Maret et al., 1979). The apo-E used in these studies had less than 0.3% of the catalytic activity of native enzyme. Careful addition of 2 mol of Zn^{2+}/80 000 daltons to the apo-E gives an essentially quantitative restoration of catalytic activity (Maret et al., 1979). Similarly high yields of the Co(II)E are obtained upon addition of Co^{2+} (Dietrich et al., 1979; Maret et al., 1979).

Stoichiometry, Thermodynamics, and Fluorescence Properties of the LADH(NAD$^+$–(Z)-DMOX) Complex. Titration of the Zn(II)E either by varying NAD$^+$ with [(Z)-DMOX] ≫ [LADH] (data not shown) or by varying (*Z*)-DMOX with [NAD$^+$] ≫ [Zn(II)E] (Figure 5) yielded plots indicating that both NAD$^+$ and (*Z*)-DMOX are bound with rather high affinities (i.e., with apparent K_D values <10 nM). The titration end points (the abscissa values at the intersection of the extrapolated linear portions of the plots) correspond to a stoichiometry of one complex per active site. The titration end points gave active site concentrations identical (within the limits of experimental error) with the values obtained via either the pyrazole–NAD$^+$ titration (Theorell & Yonetani, 1963) or the isobutyramide–NADH titration (Sund & Theorell, 1963).

The binding of NAD$^+$ to Zn(II)E partially quenches the intrinsic fluorescence of the native protein. Reaction of (*Z*)-DMOX with the Zn(II)E(NAD$^+$) complex brings about nearly complete quenching of the residual protein fluorescence, thereby providing a sensitive signal for titrating dilute enzyme samples (Figure 5). The LADH(NAD$^+$–(*Z*)-DMOX) complex (data not shown) is weakly fluorescent (λ_{ex}^{max} 430 nm;

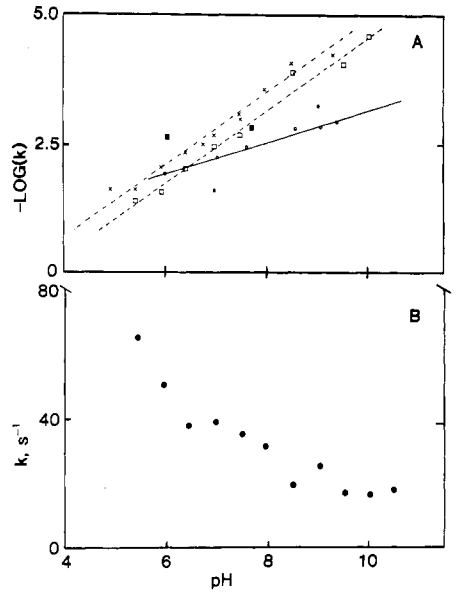

FIGURE 6: pH dependencies of apparent first-order rate constants of (*Z*)-DMOX dissociation from the Zn(II)-, Co(II)-, Ni(II)-, Cd(II)-, and Cu(II)E(NAD$^+$–(*Z*)-DMOX) ternary complexes (A) and from the apo-E(NAD$^+$–(*Z*)-DMOX) complex (B) at 25.0 ± 0.2 °C. (A) Zn(II)E (□) (– –); Co(II)E (+) (–·–); Ni(II)E (○) (—); Cd(II)E (■); Cu(II)E (●). Buffers were (pH 4–6.6) 0.1 M potassium–MES, (pH 6.7–8.1) 0.1 M potassium–TES, (pH 8.2–8.8) 0.1 M solution pyrophosphate, and (pH 8.9–10.5) 0.2 M potassium glycinate, all at 25.0 °C. Apparent first-order rate constants were determined from time courses measured at 460 nm (see Materials and Methods). (B) Apparent first-order rate constants (k) for the dissociation of (*Z*)-DMOX from the apo-E(NAD$^+$–(*Z*)-DMOX) complex were determined from time courses measured at 412 nm with a rapid-mixing stopped-flow spectrophotometer by mixing apo-E, NAD$^+$, and (*Z*)-DMOX premixed in one syringe with a pyrazole solution in the other syringe. Conditions after mixing were as follows: $[\text{apo-E}]_0$ = 17.5 μN; $[(Z)\text{-DMOX}]_0$ = 13.9 μM; $[\text{NAD}^+]_0$ = 1.14 mM; $[\text{pyrazole}]_0$ = 0.208 M. Buffers were (pH 5.0–6.6) 0.1 M potassium–MES, (pH 6.7–8.3) 0.1 M potassium–TES, (pH 8.4–8.8) 0.1 M sodium pyrophosphate, (pH 8.9–10.2) potassium glycinate, and (pH >10.2) 0.1 M potassium carbonate.

λ_{em}^{max} 505 nm). Titrations monitored either via the quenching of protein fluorescence or via the fluorescence of bound (*Z*)-DMOX give signals that are proportional to the amount of (*Z*)-DMOX bound. The titration end points give enzyme site concentrations essentially identical (±10%) with the values determined via the IBA–NADH titration.

Kinetic Studies. Kinetic studies of the reaction of DMOX with the Zn(II)E(NAD$^+$) complex were carried out by using stopped-flow rapid-mixing spectrophotometric techniques. Under the conditions of $[\text{NAD}^+] \gg [\text{Zn(II)E}] \gg [(Z)\text{-DMOX}]$, the complex is formed in a moderately rapid, apparent first-order reaction. When $[\text{Zn(II)E}]_0$ = 30.9 μN, $[\text{NAD}^+]_0$ = 0.5 mM, and $[(Z)\text{-DMOX}]_0$ = 3.62 μM, the reaction occurs with an observed rate constant of ~12 s^{-1} (in 10 mM pH 8.75 sodium pyrophosphate buffer, 25.0 ± 0.2 °C). Under other conditions (i.e., when $[\text{NAD}^+]$, $[(Z)\text{-DMOX}] \gg [\text{Zn(II)E}]$), the reaction time course consists of two kinetic phases, indicating the mechanism of the reaction is complex.

The kinetics of the displacement of (*Z*)-DMOX from the ternary complexes by excess pyrazole (Figure 6) were investigated as a function of pH both to determine the effects of metal ion substitution on the rate of (*Z*)-DMOX dissociation (Figure 6A) and to probe the differences between the ternary complexes involving apo-E and the metal ion substituted enzymes (Figure 6B). The reaction time courses were measured by following the decay of the red-shifted spectral bands after addition of high concentrations of pyrazole. Measurements were made at 460 and at 412 nm for metal-substituted and apoenzyme complexes, respectively. In these reactions, pyrazole displaces the oxime forming the LADH(NAD$^+$–pyrazole) complex:

$$\text{LADH(NAD}^+\text{–(}Z\text{)-DMOX)} \underset{k_{on}}{\overset{k_{off}}{\rightleftharpoons}} \text{LADH(NAD}^+\text{)} + (Z)\text{-DMOX}$$

$$\text{LADH(NAD}^+\text{)} + \text{pyrazole} \xrightarrow{k_2} \text{LADH(NAD}^+\text{–pyrazole)} \quad (2)$$

Under conditions of high pyrazole concentration where step k_2 is made quasi-irreversible and rapid relative to both k_{off} and k_{on}, k_{off} becomes rate determining. At high pyrazole concentrations, the apparent first-order rate constants were found to be independent of the pyrazole concentration. The pH dependencies of these rate constants are summarized in Figure 6A. At all pH values investigated, the decay process is very slow (10^{-2}–10^{-4} s^{-1}) for the metal ion substituted enzymes. The rates decrease with increasing pH (Figure 6A), and the plots of log k_{obsd} vs. pH for the Co(II) and Zn(II) derivatives are linear with slopes of approximately −0.72 and −0.68, respectively, indicating the rate of dissociation is essentially first order with respect to the concentration of hydrogen ion. The two data points for the Cu(II) derivative also indicate a first-order dependence on hydrogen ion. The plots for the Cd(II)– and Ni(II)–enzymes with slopes of −0.31 indicate a more complex dependence.

Pyrazole also forms a ternary complex with apo-E and NAD$^+$ (Dietrich et al., 1983). Figure 6B shows the pH dependence of the decay rates for the displacement of (*Z*)-DMOX from the apo-E(NAD$^+$–(*Z*)-DMOX) complex by pyrazole. At high pH, the rate of (*Z*)-DMOX dissociation (~15 s^{-1}) is independent of pH. As the pH is lowered, the rate increases to values ≥65 s^{-1}. The pH dependence shown in Figure 6B suggests the apparent pK_a for this transition is <6. Figure 6 shows that (*Z*)-DMOX dissociates from the apo-E complex with apparent rates that are 3–4 orders of magnitude faster than the rates found for the metal-substituted species.

Model Studies. It was of interest to examine the spectral properties of model compounds in which the "oxime-like nitrogen" carries a formal positive charge. The nitrone, *N*-phenyl-α-[2-[4-(dimethylamino)phenyl]ethenyl]nitrone (structures I and II), proved to be a suitable spectroscopic model (see Discussion). The ^{1}H NMR of the nitrone indicates the presence of both the *Z* and *E* isomers (structures I and II). The UV–visible spectrum of this mixture is characterized by a long-wavelength π,π* spectral band with an apparent $\lambda_{max}^{ethanol}$ of 436 nm and apparent ϵ_{max} of 3.8 × 10^4 M^{-1} cm^{-1}.

The spectral changes accompanying coordination of (*Z*)-DMOX to Zn^{2+} and Ni^{2+} in acetonitrile solution (data not shown) also were investigated. When (*Z*)-DMOX is added to a nearly saturated acetonitrile solution of $Zn(NO_3)_2$, the spectrum of (*Z*)-DMOX ($\lambda_{max}^{CH_3CN}$ 354 nm) is red-shifted to a λ_{max} of 383 nm. Addition of (*Z*)-DMOX to a saturated solution of $NiCl_2$ in CH_3CN gave a smaller apparent red-shift. Owing to the lower solubility of $NiCl_2$ in CH_3CN and to the apparent weak affinity of Ni^{2+} for (*Z*)-DMOX under these conditions, the spectrum of the Ni(II)-coordinated (*Z*)-DMOX was not resolved from that of free (*Z*)-DMOX.

Discussion

Only the *Z* isomer of DMOX reacts with enzyme-bound oxidized coenzyme to form a ternary complex at each site in

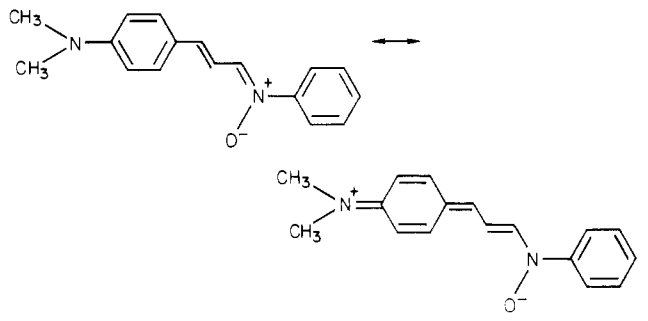

I, *Z* isomer

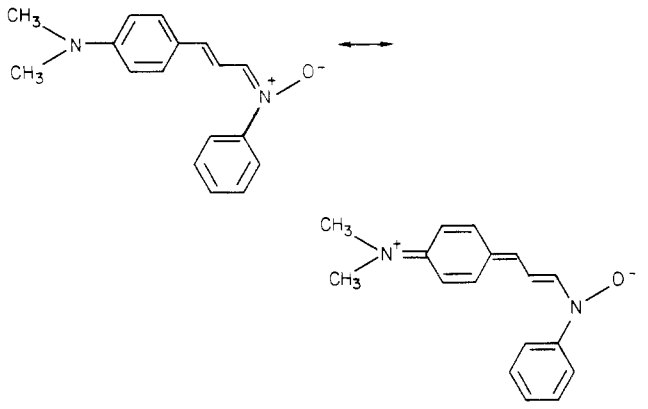

II, *E* isomer

which the spectrum of the (*Z*)-DMOX chromophore is red-shifted ~80 nm (Figure 1). The apparently absolute specificity for the *Z* isomer of DMOX is in agreement with the findings of Sigman et al. (1982) for aliphatic oximes. The λ_{max} and ϵ_{max} of the long-wavelength absorption bands for all the complexes (Table II) are insensitive to the nature of the substituent on the pyridinium ring of the analogue.

The high affinity of the Zn(II)E(NAD$^+$) complex for (*Z*)-DMOX (viz., Figure 5) indicates an apparent dissociation constant for (*Z*)-DMOX of <10 nM at pH 8.75. The sharp end points in these titrations demonstrate a stoichiometry of 1 mol of (*Z*)-DMOX bound/mol of enzyme site. The rate of complex formation when Zn(II)E and NAD$^+$ are in excess of (*Z*)-DMOX yields an estimated association rate constant (k_1) of $\geq 4 \times 10^5$ M^{-1} s^{-1} at pH 8.75. Displacement by pyrazole at this pH gives an estimated dissociation rate constant (k_{-1}) of 9.3×10^{-4} s^{-1}. The ratio k_{-1}/k_1 yields an apparent dissociation constant of ~2.3 nM. The computer simulation of the fluorescence quenching titration (Figure 5) indicates a value of ~4 nM. Sigman et al. (1982) report a value of 5.56 nM at pH 7.0. The excellent absorption and fluorescence spectroscopic properties of the complex and the high affinity make (*Z*)-DMOX a potentially useful active site titrant for the determination of LADH active site concentrations. The spectroscopic advantages of the (*Z*)-DMOX system are partially offset by the instability of the *Z* isomer. In aqueous solution, the *Z* isomer undergoes a slow conversion (probably light catalyzed) to the thermodynamically more stable but inactive *E* isomer. The crystalline material is stable in the dark when stored at 4 °C for time periods ≥2 years.

Evidence for Adduct Formation between (Z)-DMOX and Coenzyme. The spectra of the NAD$^+$, 3-acetyl-PdAD$^+$, and 3-thio-NAD$^+$ ternary complexes with (*Z*)-DMOX each contain a second, higher energy, absorption band (Figure 1 and Table II). This electronic transition was not detected in the io^{3}PdAD$^+$ complex (viz., Figure 1D). On the basis of the spectral properties of io^{3}PdADH (Table IV), it is probable that in the io^{3}PdAD$^+$ complex this transition occurs at higher energy and, therefore, is obscured in the spectrum by the absorbancies of the enzyme, io^{3}PdAD$^+$, and (*Z*)-DMOX. The difference spectrum for the NMN$^+$ system in the 290–300-nm region (Figure 2) suggests the presence of a second transition at ~290 nm.

The λ_{max} of the second absorption bands for the NAD$^+$, 3-acetyl-PdAD$^+$, and 3-thio-NAD$^+$ complexes (respectively, 280, 305, and 335 nm; viz., Table II) appears to reflect the nature of the substituent at the 3-position of the coenzyme pyridine ring (Table IV). Therefore, we conclude that these absorption bands are derived from electronic transitions associated with the π systems of these pyridine rings. We further conclude that these spectral bands arise from the corresponding dihydropyridine structures derived from adduct formation between (*Z*)-DMOX and the coenzyme (Scheme I). Structures involving either bonding to the nicotinamide ring via the oxime nitrogen with the oxime oxygen coordinated to zinc (structure III) or bonding to the nicotinamide ring via the oxime oxygen with the oxime nitrogen coordinated to zinc (structure IV) are shown. Although the corresponding 2- and 6-adducts cannot be ruled out, 4-adducts are shown here by analogy to the X-ray structure of the LADH(NAD$^+$–pyr) adduct (Eklund et al., 1982). In agreement with this assignment, Sigman et al. (1982) have shown that the reaction of aliphatic oximes with the LADH(NAD$^+$) complex gives ternary complexes that exhibit a new absorption band between 290 and 305 nm. Since both hydroxylamine and *N*-methylhydroxamine form ternary complexes with absorption bands in this region while *O*-methylhydroxylamine does not, they also assign this spectral band to the formation of an adduct between the oxime oxygen and the nicotinamide ring of NAD$^+$. If adducts are formed, then the corresponding reduced coenzymes should be good spectroscopic analogues. This prediction is borne out by the data summarized in Table IV; the spectra of the C-4-reduced coenzymes, the cyanide adducts, and the hydroxylamine adducts all have λ_{max} values that exhibit dependencies on the nature of the substituent at the 3-position of the ring that are similar to those of the DMOX complexes. Assuming that the same bonding interactions occur in the io^{3}PdAD$^+$ complex, the electronic transition derived from the pyridine ring moiety should occur below 280 nm (Abdallah et al., 1976; Abdallah & Biellmann, 1980), a region we could not examine in these experiments.

The relatively low affinity of the E(io$^+$PdAD$^+$) complex for (*Z*)-DMOX very likely has its origins in the predominance of a binary complex in which the pyridine riboside portion of the coenzyme is directed back toward the surface of the protein rather than toward the active site zinc ion (Abdallah et al., 1976; Samama et al., 1977; Ekland et al., 19871). We postulate that reaction with (*Z*)-DMOX drives the pyridine ring of io^{3}PdAD$^+$ into the nicotinamide subsite, thus making possible the bonding of (*Z*)-DMOX both to io^{3}PdAD$^+$ and to Zn^{2+} in the ternary complex.

NMN$^+$ binds only very weakly if at all to the nicotinamide subsite (NMN$^+$ binds preferentially to the AMP subsite; Sigman, 1967; Schmid et al., 1978). The formation of an E(NMN$^+$–(*Z*)-DMOX) complex with $\lambda_{max} \simeq 430$ nm (Figure 2) indicates that bonding of (*Z*)-DMOX to the nicotinamide ring stabilizes the binding of NMN$^+$ in the nicotinamide subsite.

Chemical Nature of the (Z)-DMOX Ternary Complex. The reaction of 4-*trans*-(*N*,*N*-dimethylamino)cinnamaldehyde (DACA) with the LADH(NADH) complex results in the formation of a transient intermediate exhibiting a similarly red-shifted spectrum (Dunn & Hutchison, 1973; Dunn et al.,

Table IV: Comparison of the UV-Visible Spectral Properties of Enzyme-Bound Nucleophile–NAD$^+$ Adducts with the Spectra of the 1,4-Reduced Analogues

NAD$^+$ analogue	λ_{max} (nm) of LADH ternary complexes with (*Z*)-DMOX	CN-[a]	NH_2OH[a]	NADH analogue	λ_{max} (nm) of LADH binary complexes with 1,4-reduced analogues[a]	λ_{max} (nm) of free 1,4-reduced analogues[a]
NAD^+	290 428	310	300	NADH	325	340
3-acetyl-$PdAD^+$	305 432	340[d]	325	3-acetyl-PdADH	350	363
3-thio-NAD^+	335 428	335[b]		3-thio-NADH	387[e]	395
io^3PdAD^+[c]	427	262		io^3PdADH[c]	*f*	259
NMN^+	430			NMNH	*f*	340

[a] Sund & Theorell (1963). [b] Pabst Laboratories Circular OR-18 (1965). [c] Abdallah et al. (1976). Note that io^3PdAD^+ has $\lambda_{max}^{H_2O}$ 255 nm (~1.8×10^4 M^{-1} cm^{-1}) and a shoulder at 295 nm (~2.5×10^3 M^{-1} cm^{-1}) and io^3PdADH has $\lambda_{max}^{H_2O}$ 259 nm (~1.7×10^4 M^{-1} cm^{-1}). [d] Kaplan (1960). [e] For the ternary E(3-thio-NADH-IBA) complex, Joppich-Kuhn & Luisi (1978). [f] Not reported.

Scheme I

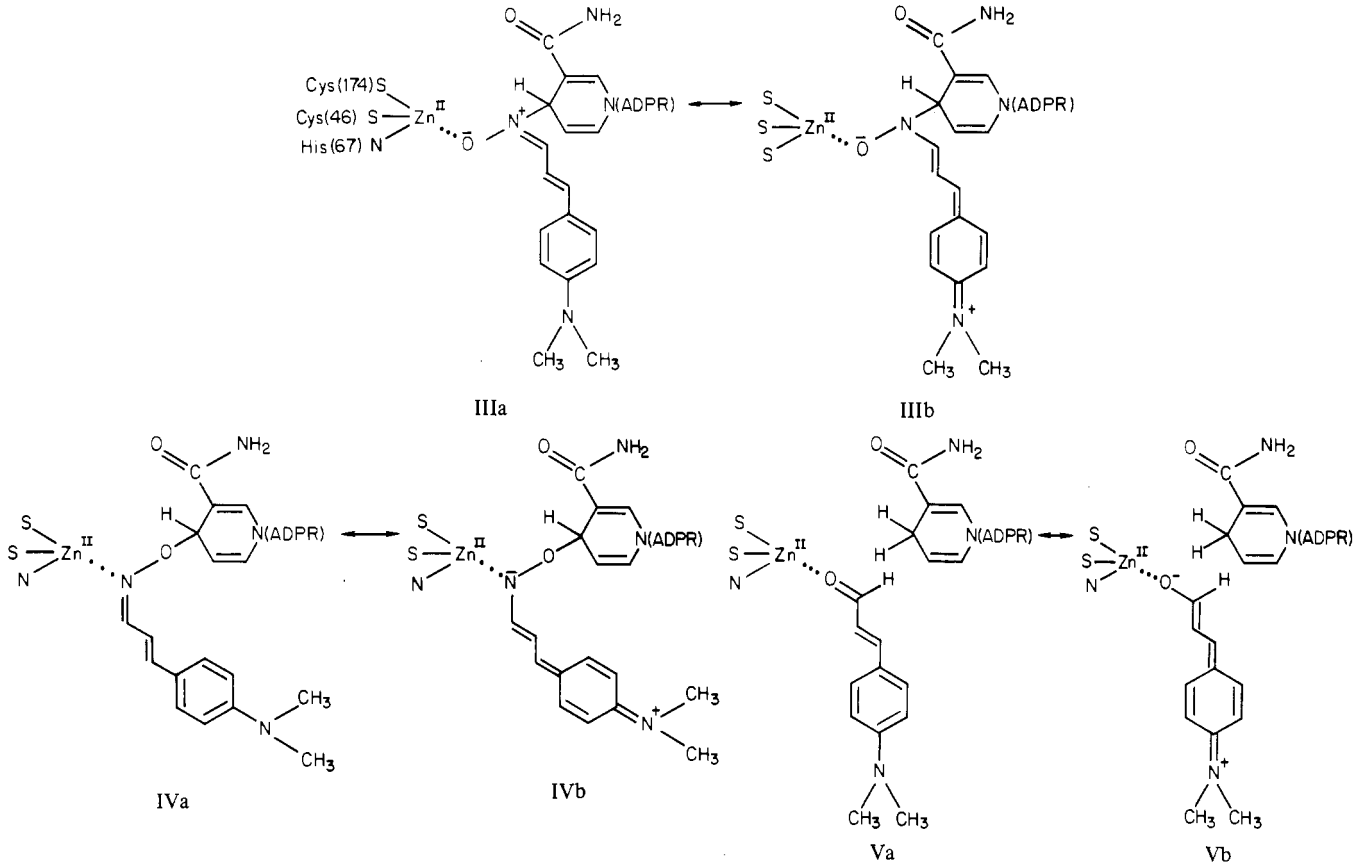

1975, 1982; Morris et al., 1980). The DACA spectral changes originate from inner sphere coordination of the carbonyl oxygen of DACA to the active site zinc ion [see structure V of Scheme I (Dunn & Hutchison, 1973; Dunn et al., 1975, 1982; Angelis et al., 1977; Dietrich et al., 1979; Cedergren-Zeppezauer et al., 1982)]. However, since the LADH(NAD^+) complex contains two powerful electrophiles, NAD^+ and Zn^{2+}, bonding interactions to either NAD^+ or Zn^{2+} via the oxime nitrogen (viz., structures III and IV of Scheme I) could account for the red-shifted spectra of Figures 1–3.

The Cu(II)–, Ni(II)–, and Co(II)–enzymes exhibit spectral bands attributable to metal–sulfur charge-transfer interactions in the region 300–430 nm for Co(II) and Ni(II) and in the region 500–800 nm for Cu(II). The Co(II)–enzyme exhibits d–d electronic transitions in the 500–700-nm region. The 300–430-nm charge-transfer transitions of these derivatives are partially obscured by the intense π,π^* transitions of bound (*Z*)-DMOX. However, the long-wavelength transitions of the Co(II)E (Figure 3A) and the Cu(II)E (Figure 3B) are free from other interfering spectral bands. The spectra in Figure 3 show that formation of the (*Z*)-DMOX ternary complex causes shifts in the d–d transitions of both λ_{max} and ϵ.

Maret et al. (1979, 1982), Dietrich et al. (1979), Maret et al. (1981), Dietrich & Zeppezauer (1982), and Koerber et al. (1983) have shown that the visible spectra of the Co(II)– and Cu(II)–enzymes are sensitive probes of ligand binding both to the substrate site and to the coenzyme site. The spectral changes of both the (*Z*)-DMOX chromophore and of the d–d and LMCT transitions associated with ternary complex formation (Figure 3) are consistent with the direct coordination of (*Z*)-DMOX both to Co(II) and to Cu(II), respectively, in these enzyme derivatives. The remarkable dependence of the (*Z*)-DMOX dissociation rate constants on the presence of a divalent metal ion at the site, compare apo-E (Figure 6B) with the metalloenzyme derivatives (Figure 6A), also is consistent with direct coordination in the metal ion substituted enzyme derivatives. The remaining question concerns the identity of the atom (oxime nitrogen or oxygen) that coordinates to the

metal atom and that atom bonds to the C-4 of the nicotinamide ring.

To investigate the steric constraints imposed by the active site of the enzyme and the possible modes of adduct formation, we undertook computer-assisted model-building exercises to determine which orientations and bonding interactions are likely possibilities for the E(NAD$^+$–(*Z*)-DMOX) complex. By use of the refined atomic coordinates for the triclinic LADH-(NADH, Me_2SO) structure (H. Eklund, private communication), the following constraints were imposed: (1) no structural changes were allowed in the protein or NADH models; (2) the bond distance between the active site Zn^{2+} atom and the liganding atom from (*Z*)-DMOX is 2.0 Å; (3) the constellation of atoms consisting of (*Z*)-DMOX, Zn^{2+}, and the C-4 carbon of NAD$^+$ defines a plane; (4) the O–N–C oxime angle is ~115° (an average of literature values taken from the X-ray structures of oximes and oxime–metal ion complexes; Wetherington & Moncreif, 1973; Godycke & Rundle, 1955; Williams et al., 1959; Stone et al., 1971; Ginderow, 1975).

The results are summarized in Scheme II. With these constraints, the most reasonable structure found involves coordination of the oxime nitrogen to zinc. With a 2.0-Å N–Zn distance, van der Waals contacts between the binding cleft and the (*N*,*N*-dimethylamino)phenyl portion of (*Z*)-DMOX limited the distance between the oxime oxygen and the 4-carbon of the nicotinamide ring to ~2.0 Å (structure A, Scheme II). In structure A, the only unacceptably short van der Waals contacts occur between (*Z*)-DMOX and Met-306 (from the other subunit). If the S–CH_3 group of Met-306 is allowed to rotate to a new position, then the fit between (*Z*)-DMOX and the site is satisfactory. X-ray structure studies of the E(H_2NADH,DACA) complex (Cedergren-Zeppezauer et al., 1982) show that the S–CH_3 group of Met-306 is located in an alternative position [presumably to accommodate the –N-$(CH_3)_2$ group of DACA]. The distance between the oxime oxygen and the 4-carbon of the ring in structure A could be shortened by a slight rotation of the nicotinamide ring about the glycosidic C–N bond. Due to spatial constraints imposed by the site, it was found that complexes involving coordination of the oxime oxygen, covalent bonding to the nicotinamide ring via the oxime nitrogen, and acceptable van der Waals contacts could not be fit into the site. Our efforts gave structures (viz., structure B) in which the *best fit* bond distance between the oxime nitrogen and the NAD$^+$ 4-carbon is too long for a covalent bond (i.e., ≤2 Å). These complexes were also characterized by unacceptably short van der Waals contacts between the $(CH_3)_2$N group of (*Z*)-DMOX, Leu-116, Phe-140, and Leu-141 (i.e., <2.2 Å). To achieve a fit of structure B with acceptable bond lengths, bond angles, and van der Waals contacts, the tertiary structure of the catalytic domain in the vicinity of the substrate binding site must be significantly different from that of the E(NADH,Me_2SO) complex.[2] Thus, these model-building studies strongly suggest that the bonding interactions between (*Z*)-DMOX, the active site zinc ion, and the nicotinamide ring occur as depicted in structure A with coordination via the oxime nitrogen and covalent bonding to the ring 4-position. Sigman et al. (1982) propose a similar mode of bonding both for aliphatic oximes and for (*Z*)-DMOX. The X-ray structures of oxime complexes with divalent transition metal ions show that bonding occurs via inner sphere coordination of the oxime nitrogen in all examples reported (Williams et al., 1959; Godycke & Rundle, 1955; Stone et al., 1971).

The formation of a red-shifted ternary complex with the apo-E and NAD$^+$ (Figure 4) with spectral properties at pH 7.5 that are closely similar to the complexes formed with the

Scheme II: Structural Models Depicting the Steric Constraints Imposed on the Reaction of (*Z*)-DMOX with the E(NAD$^+$) Complex[a]

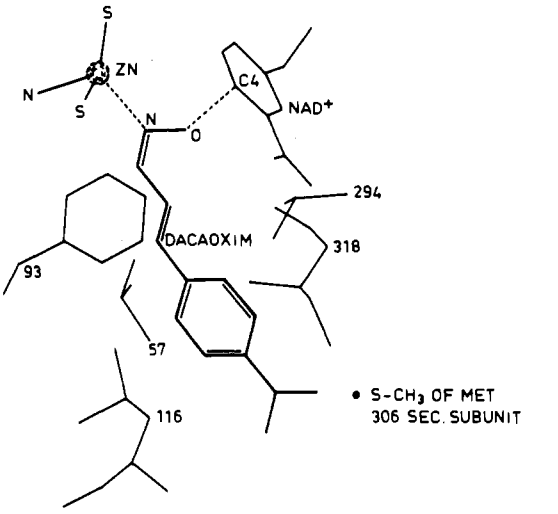

A

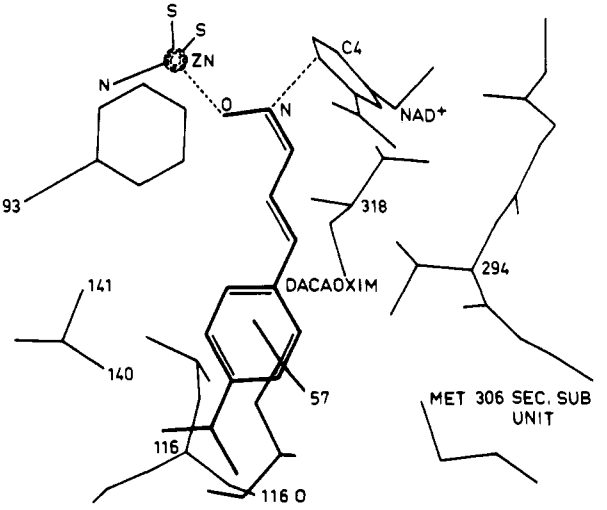

B

[a] The protein and coenzyme coordinates are derived from the 2.5-Å resolution structure of the triclinic E(NADH,Me_2SO) complex. The active site zinc atom is indicated by a dotted sphere bonded to the three protein ligands (the sulfurs of Cys-46 and Cys-176 and the 2-imidazolyl nitrogen of His-67). A fourth bond drawn to the oxime moiety of (*Z*)-DMOX (via nitrogen in structure A and via oxygen in structure B) completes a roughly tetrahedral coordination sphere. In these "cutaway" views, the best possible fits of (*Z*)-DMOX to the hydrophobic substrate binding cleft are shown (see text). (Structure A) (*Z*)-DMOX oxime nitrogen is liganded to zinc with an N–Zn bond length of 2.0 Å. The oxime oxygen–NAD$^+$ C-4 distance is 1.9 Å. In this "best fit", the only unfavorable van der Waals contacts involve the -$N(CH_3)_2$ group of DACA and Met-306. (Structure B) Oxime oxygen is liganded to zinc with an O–Zn bond length of 2.0 Å. In this "best fit" orientation, the oxime nitrogen is >2.0 Å from the C-4 carbon of NAD$^+$, while the -$N(CH_3)_2$ group of DACA makes unacceptably short van der Waals contacts with Leu-116, Phe-140, and Leu-141.

[2] Preliminary crystallographic studies show that the E(NAD$^+$–(*Z*)-DMOX) complex crystallizes in the same space group $P2_1$ with the dimeric molecule in the asymmetric unit. This crystal form represents an enzyme structure similar to the triclinic E(NADH,Me_2SO) complex used as the reference structure in the model studies.

Scheme III

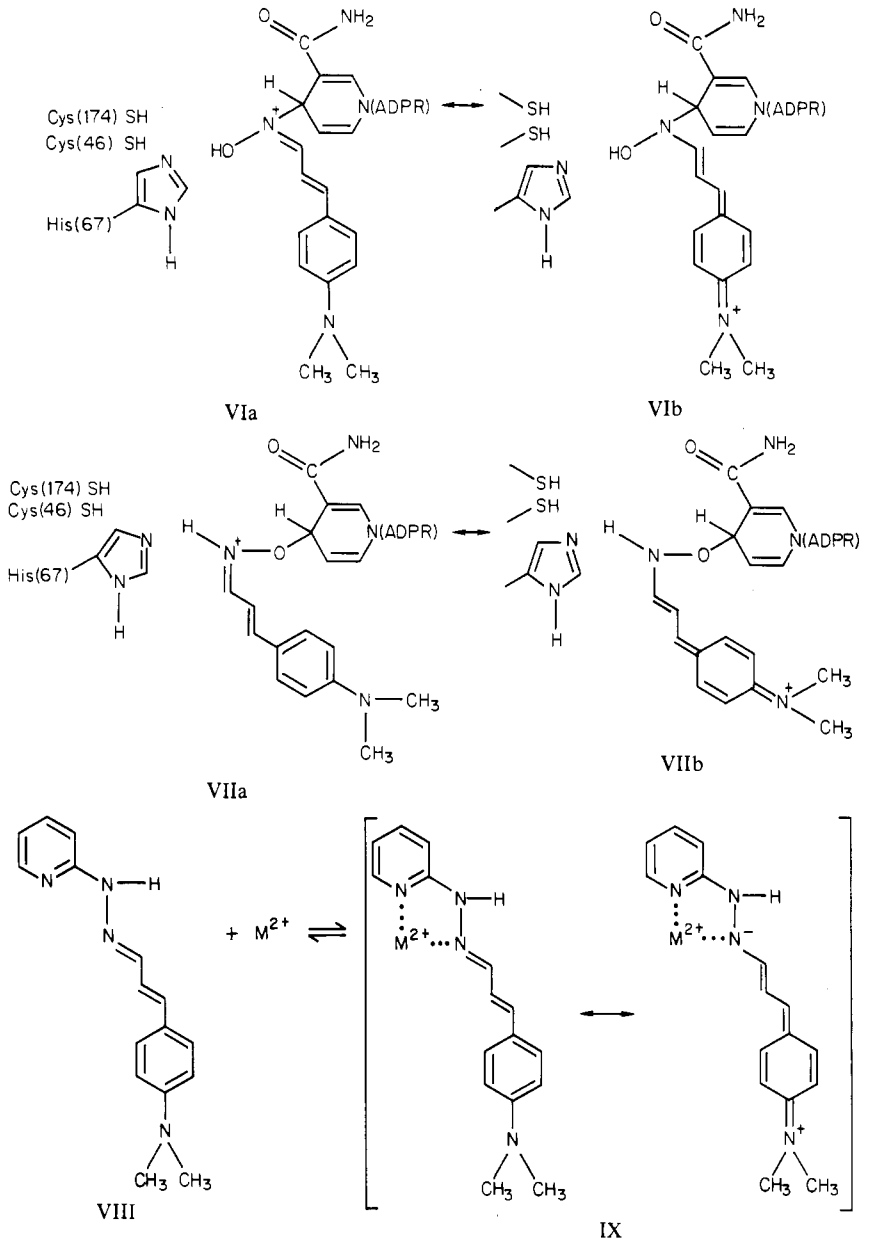

metalloenzyme derivatives demonstrates that, for this enzyme derivative, bonding to some electrophilic center other than the active site metal ion is responsible for the red-shift. The red-shifted spectrum of the apo-E ternary complex must arise either via bonding of the oxime nitrogen to the nicotinamide ring (Scheme III, structure VI) or via substitution of a new electrophilic center for the missing zinc ion, e.g., a proton (viz., structure VII). Such centers are created by protonation of His-67, Cys-46, and Cys-174 upon removal of the catalytic metal ion (Schneider & Zeppezauer, 1983; Schneider et al., 1983).

The pH-dependent spectrum of the apo-E(NAD$^+$–(*Z*)-DMOX) complex, almost certainly, is due to the ionization of a protonated component of the complex, either (*Z*)-DMOX or a protein residue in close proximity to the (*Z*)-DMOX chromophore. Protonation of the oxime nitrogen (structure VII) would shift the spectrum of (*Z*)-DMOX to the red. Ionization of this protonated species would convey a pH dependence to the spectrum of the complex. Conversely, if the red-shifted spectrum of the apo-E complex arises from bonding of the oxime nitrogen to the nicotinamide ring (structure VI), then the pH dependence of the spectrum must result from either the ionization of the oxime hydroxyl or of a nearby protein residue (e.g., Cys-46 or Cys-174).

Comparisons with Other Systems. Model studies of close structural analogues of (*Z*)-DMOX (Angelis et al., 1977) have demonstrated that bonding interactions involving the imine nitrogen of the chromophore that result in electron withdrawal, i.e., metal ions (structure IX), alkylation, or arylation (structure I), cause similarly large red-shifts in the π,π^* transition (viz., Table III).

Direct comparison of the effects of Lewis acid strength on the spectral shifts is made difficult by differences in coordination geometry and coordination number; the Zn(II) complex is tetrahedral (Angelis et al., 1977), the Co(II) complex probably is tetrahedral, the Cu(II) and Ni(II) complexes almost undoubtedly are square planar (Holm & O'Connor, 1971), and the Cd(II) complex probably has a coordination number >4.

In contrast to model systems, solution spectroscopic and X-ray crystallographic studies of the metal-substituted LADH catalytic site indicate a distorted tetrahedral ligand field that is highly conservative with respect to coordination number and geometry of the substituted metal atom (Zeppezauer, 1983;

Schneider et al., 1983; G. Schneider et al., unpublished results). A recent X-ray analysis of 2.4-Å resolution has shown that the tertiary structure of Co(II)–LADH is virtually indistinguishable from that of the native enzyme. Most important, the position and distance of the metal ligands, including the metal-bound water molecule remain the same within narrow limits (Schneider et al., 1983). Also, Cd(II)–LADH (G. Schneider et al., unpublished results), which was studied at 2.9-Å resolution, remains four-coordinated, although slight changes in the positions of the metal binding side chains are observed as a consequence of the significantly larger ionic radius of Cd(II) as compared to that of Zn(II). By inference, we may expect even the Ni(II), Cu(II), and other metallo derivatives to conserve a four-coordinate, tetrahedral catalytic metal binding site.

Table III shows that the spectral shifts associated with the formation of the (*Z*)-DMOX complexes, although generally slightly larger, are similar in magnitude to the red-shifts that accompany the reaction of 4-*trans*-(*N*,*N*-dimethylamino)-cinnamaldehyde (DACA) with the metal-substituted LADH-(NADH) complexes (60–80 nm; Dunn & Hutchison, 1973; Dietrich et al., 1979; Dunn et al., 1981). DACA does not form red-shifted ternary complexes with apo-E(NADH) or with apo-E(NAD^+). The (*Z*)-DMOX reaction is also highly specific; (*Z*)-DMOX does not form red-shifted complexes with either apo-E(NADH) or the metal ion substituted E(NADH) complexes (Zn^{2+} included). These observatives are consistent with the differences in modes of bonding proposed for the two types of complexes (viz., structures III and IV vs. structure V).

In comparison to the relatively unfavorable reactions of free NAD^+ with nucleophiles in aqueous solution, the highly favorable nature of the reactions of (*Z*)-DMOX and other nucleophiles with enzyme-bound NAD^+ undoubtedly is a consequence of the entropic advantages arising from the "intramolecular" character of adduct formation within the ternary complex (Jencks, 1975; Bruice & Benkovic, 1966). Just as in the catalytic reaction where coordination of alcohol undoubtedly places the C-1 hydrogen of the substrate within bonding distance of the C-4 of NAD^+, the binding and coordination of (*Z*)-DMOX to the active site metal ion orients the oxime for nucleophilic attack on the nicotinamide ring via a "template effect" (Dunn, 1975).

Acknowledgments

We are indebted to Dr. Hans Eklund for providing us with the refined coordinates of the triclinic LADH(NADH,Me_2SO) complex before publication and to Dr. Horjales for his valuable assistance in the model-building studies. We thank David Murray, Steven Arndt, and Dr. P. K. Chattopadhyay for their contributions to this work at early stages of the project, and we thank Professor David Sigman and Dr. Marianne Frölich for making available to us the results of their work on the DMOX reaction prior to publication. We thank Professor Judy Klinman for stimulating discussions relevant to this work. And we thank E. Krempp, P. E. Maltese, R. Graff, and F. Hemmert for carrying out the NMR studies.

Registry No. (*Z*)-DMOX, 88425-12-1; (*E*)-DMOX, 88425-13-2; DACA, 20432-35-3; CDI, 530-62-1.

References

Abdallah, M. A., & Biellmann, J.-F. (1980) *Eur. J. Biochem. 112*, 331–333.

Abdallah, M. A., Biellmann, J.-F., Samama, J.-P., & Wrixon, A. D. (1976) *Eur. J. Biochem. 64*, 351–360.

Andersson, I. (1980) Dissertation, Universität des Saarlandes, Saarbrücken, West Germany.

Andersson, P., Kvassman, J., Lindström, A., Oldén, B., & Pettersson, G. (1981) *Eur. J. Biochem. 114*, 549–554.

Angelis, C. T., Dunn, M. F., Muchmore, D. C., & Wing, R. W. (1977) *Biochemistry 16*, 2922–2931.

Bernhard, S. A., Dunn, M. F., Luisi, P. L., & Schack, P. (1970) *Biochemistry 9*, 185–192.

Boyland, E., & Nery, R. (1963) *J. Chem. Soc.*, 3141–3144.

Brändén, C.-I., Jörnvall, H., Eklund, H., & Furugren, B. (1975) *Enzymes, 3rd Ed. 11*, 103–190.

Bruice, T. C., & Berkovic, S. (1966) in *Bioorganic Mechanisms*, Vol. I, pp 119–125, W. A. Benjamin, New York.

Cedergren-Zeppezauer, E., Samama, J.-P., & Eklund, H. (1982) *Biochemistry 21*, 4895–4908.

Chakrabarti, J. K., & Hotten, T. M. (1972) *J. Chem. Soc., Chem. Commun.*, 1226–1227.

Clive, D. L. J. (1970) *J. Chem. Soc. D*, 1014–1015.

Crêpeaux, D., & Lehn, J. M. (1975) *Org. Magn. Reson. 5*, 524–526.

Dietrich, H. (1980) Dissertation, Universität des Saarlandes, Saarbrücken, West Germany.

Dietrich, H., & Zeppezauer, M. (1982) *J. Inorg. Biochem. 17*, 227–235.

Dietrich, H., Maret, W., Wallén, L., & Zeppezauer, M. (1979) *Eur. J. Biochem. 100*, 267–270.

Dietrich, H., Maret, W., Kozlowski, H., & Zeppezauer, M. (1981) *J. Inorg. Biochem. 14*, 297–311.

Dietrich, H., MacGibbon, A. K. H., Dunn, M. F., & Zeppezauer, M. (1983) *Biochemistry 22*, 3432–3438.

Dunn, M. F. (1975) *Struct. Bonding (Berlin) 23*, 61–122.

Dunn, M. F., & Hutchison, J. S. (1973) *Biochemistry 12*, 4882–4892.

Dunn, M. F., Biellmann, J.-F., & Branlant, G. (1975) *Biochemistry 14*, 3176–3188.

Dunn, M. F., Bernhard, S. A., Anderson, D., Copeland, A., Morris, R. G., & Roque, J.-P. (1979) *Biochemistry 18*, 2346–2354.

Dunn, M. F., Dietrich, H., MacGibbon, A. K. H., Koerber, S. C., & Zeppezauer, M. (1982) *Biochemistry 21*, 354–363.

Eklund, H., Samama, J.-P., Wallén, L., Brändén, C.-I., Åkeson, Å., & Jones, T. W. (1981) *J. Mol. Biol. 146*, 561–587.

Eklund, H., Samama, J.-P., & Wallén, L. (1982) *Biochemistry 21*, 4858–4866.

Foley, H. G., & Dalton, D. R. (1973) *J. Chem. Soc., Chem. Commun.*, 628–629.

Frölich, M. (1977) Doctoral Dissertation, University of California, Los Angeles, CA.

Ginderow, P. D. (1975) *Acta Crystallogr., Sect. B B1*, 1092–1094.

Godycki, L. E., & Rundle, R. E. (1955) *Acta Crystallogr. 6*, 487–494.

Hill, J. H. M., & Schomookler, L. D. (1967) *J. Org. Chem. 32*, 4025.

Holm, R. H., & O'Connor, M. J. (1971) *Prog. Inorg. Chem. 14*, 241–401.

Jencks, W. P. (1975) *Adv. Enzymol. Relat. Areas Mol. Biol. 43*, 219–410.

Jones, T. A. (1982) in *Computational Crystallography* (Sayer, D., Ed.) pp 303–317, Oxford University Press, London.

Joppich-Kuhn, R., & Luisi, P. L. (1978) *Eur. J. Biochem. 83*, 593–599.

Kaplan, N. O. (1960) *Enzymes, 2nd Ed. 3*, 105–169.

Kaplan, N. O., & Ciotti, M. M. (1954) *J. Biol. Chem. 211*, 431–445.

Kintzinger, J. P., & Lehn, J. M. (1957) *Chem. Commun.*, 660–661.
Koerber, S. C., & Dunn, M. F. (1981) *Biochimie 63*, 97–102.
Koerber, S. C., MacGibbon, A. H. K., Dietrich, H., Zeppezauer, M., & Dunn, M. F. (1983) *Biochemistry 22*, 3424–3431.
Kosower, E. M. (1962) *Molecular Biochemistry*, pp 166–220, McGraw-Hill, New York.
Maret, W. (1980) Dissertation, Universität des Saarlandes, Saarbrücken, West Germany.
Maret, W., Andersson, I., Dietrich, H., Schneider-Bernlöhr, H., Einarsson, R., & Zeppezauer, M. (1979) *Eur. J. Biochem. 98*, 501–512.
Maret, W., Dietrich, H., Ruf, H., & Zeppezauer, M. (1980) *J. Inorg. Biochem. 12*, 241.
Maret, W., Zeppezauer, M., Desideri, A., Morpurgo, L., & Rotilio, G. (1981) *FEBS Lett. 136*, 72–74.
McFarland, J. T., & Bernhard, S. A. (1972) *Biochemistry 11*, 1486–1493.
Morris, R. G., Saliman, G., & Dunn, M. F. (1980) *Biochemistry 19*, 725–731.
Pabst Laboratories Circular OR-18 (1965) Third Printing, July, Pabst Laboratories, Milwaukee, WI.
Rasmussen, H. N., Nielsen, J. R., & Schack, P. (1972) *Anal. Biochem. 50*, 642–647.
Samama, J.-P., Zeppezauer, E., Biellmann, J.-F., & Brändén, C.-I. (1977) *Eur. J. Biochem. 81*, 403–409.
Schmid, F., Hinz, H.-J., & Jaenicke, R. (1978) *FEBS Lett. 87*, 80–82.
Schneider, G., & Zeppezauer, M. (1983) *J. Inorg. Biochem. 18*, 59–70.
Schneider, G., Eklund, H., Cedergren-Zeppezauer, E., & Zeppezauer, M. (1983) *Proc. Natl. Acad. Sci. U.S.A. 80*, 5289–5293.
Shifrin, S., & Kaplan, N. O. (1960) *Adv. Enzymol. Relat. Areas Mol. Biol. 22*, 337–415.
Shore, J. D., & Gilleland, M. J. (1970) *J. Biol. Chem. 245*, 3422–3425.
Siegel, J. M., Montgomery, G. A., & Bock, R. M. (1959) *Arch. Biochem. Biophys. 82*, 288–299.
Sigman, D. (1967) *J. Biol. Chem. 242*, 3815–3824.
Sigman, D. S., Frölich, M., & Anderson, R. E. (1982) *Eur. J. Biochem. 126*, 523–529.
Stone, M. F., Robertson, B. E., & Stanley, E. (1971) *J. Chem. Soc. A*, 3632–3635.
Sund, H., & Theorell, H. (1963) *Enzymes, 2nd Ed. 7*, 26–83.
Theorell, H., & Yonetani, T. (1963) *Biochem. Z. 338*, 337–553.
Wetherington, J. B., & Moncreif, J. W. (1953) *Acta Crystallogr., Sect. B B29*, 1520–1525.
Williams, D. E., Wohlauer, G., & Rundle, R. E. (1959) *J. Am. Chem. Soc. 81*, 755–756.
Zeppezauer, M. (1983) *NATO Adv. Study Inst., Ser. C 100*, 99–122.

Relationships between the Na^+–H^+ Antiport Activity and the Components of the Electrochemical Proton Gradient in *Escherichia coli* Membrane Vesicles†

Martine Bassilana, Evelyne Damiano, and Gérard Leblanc*

ABSTRACT: The kinetics of Na^+ efflux from *Escherichia coli* RA 11 membrane vesicles taking place along a favorable Na^+ concentration gradient are strongly dependent on the generation of an electrochemical proton gradient. An energy-dependent acceleration of the Na^+ efflux rate is observed at all external pHs between 5.5 and 7.5 and is prevented by uncoupling agents. The contributions of the electrical potential ($\Delta\psi$) and chemical potential (ΔpH) of H^+ to the mechanism of Na^+ efflux acceleration have been studied by determining the effects of (a) selective dissipation of $\Delta\psi$ and ΔpH in respiring membrane vesicles with valinomycin or nigericin and (b) imposition of outwardly directed K^+ diffusion gradients (imposed $\Delta\psi$, interior negative) or acetate diffusion gradients (imposed ΔpH, interior alkaline). The data indicate that, at pH 6.6 and 7.5, ΔpH and $\Delta\psi$ individually and concurrently accelerate the downhill Na^+ efflux rate. At pH 5.5, the Na^+ efflux rate is enhanced by ΔpH only when the imposed ΔpH exceeds a threshold ΔpH value; moreover, an imposed $\Delta\psi$ which per se does not enhance the Na^+ efflux rate does contribute to the acceleration of Na^+ efflux when imposed simultaneously with a ΔpH higher than the threshold ΔpH value. The results strongly suggest that the Na^+–H^+ antiport mechanism catalyzes the downhill Na^+ efflux. Furthermore, they suggest that (a) the overall exchange reaction is rate limited by the rate of coupled H^+ influx, (b) the Na^+–H^+ antiporter might function as an electrogenic process at all pHs between 5.5 and 7.5, and finally (c) the antiport function is controlled, in particular at acidic pHs, by a ΔpH-sensitive reaction or alternatively by the internal pH.

In Mitchell's chemiosmotic hypothesis, the ionic gradients across the cytoplasmic membrane are proposed to serve the purpose both of the conservation of energy and of its transmission from energy-producing to energy-consuming membrane reactions (Mitchell, 1963, 1968, 1970). It is thus well recognized that in intact bacteria or derived membrane vesicles, the electrochemical proton gradient ($\Delta\bar{\mu}_{H^+}$)[1] (Mitchell, 1963)

† From the Laboratoire Jean Maetz, Département de Biologie, Commissariat à l'Energie Atomique associé à l'Equipe de Recherche 247 du C.N.R.S., Station Marine, B.P. 68, 06230 Villefranche-sur-Mer, France. *Received April 8, 1983; revised manuscript received September 13, 1983.*

[1] Abbreviations: $\Delta\bar{\mu}_{H^+}$, electrochemical gradient of protons; ΔpH, proton gradient across the membrane; $\Delta\psi$, electrical potential across the membrane; $\Delta\bar{\mu}_{Na^+}$, electrochemical gradient for Na^+ ions; PMS, phenazine methosulfate; FCCP, carbonyl cyanide *p*-(trifluoromethyl)phenylhydrazone; Me_2SO, dimethyl sulfoxide.

0006-2960/84/0423-1015$01.50/0